VPS VIBRATIONS IN PHYSICAL SYSTEMS

DOI: 10.21008/j.0860-6897.2023.1.06
Vibrations in Physical Systems,2023, 34(1), 2023106

Calculation strength optimum of surgical robot effector for mechanical eigenproblems using FEM and genetic algorithm

Grzegorz ILEWICZ

Warsaw University of Technology, Institute of Micromechanics and Photonics, Faculty of Mechatronics

Corresponding author: Grzegorz ILEWICZ, email: grzegorz.ilewicz@pw.edu.pl

Abstract It is essential to check whether the surgical robot end effector is safe to use due to phenomena such as linear buckling and mechanical resonance. The aim of this research is to build an multi criteria optimization model based on such criteria as the first natural frequency, buckling factor and mass, with the assumption of the basic constraint in the form of a safety factor. The calculations are performed for a serial structure of surgical robot end effector with six degrees of freedom ended with a scalpel. The calculation model is obtained using the finite element method. The issue of multi-criteria optimization is solved based on the response surface method, Pareto fronts and the genetic algorithm. The results section illustrates deformations of a surgical robot end effector occurring during the resonance phenomenon and the buckling deformations for subsequent values of the buckling coefficients. The dependencies of the geometrical dimensions on the criteria are illustrated with the continuous functions of the response surface, i.e. metamodels. Pareto fronts are illustrated, based on which the genetic algorithm finds the optimal quantities of the vector function. The conducted analyzes provide a basis for selecting surgical robot end effector drive systems from the point of view of their generated inputs.

Keywords: surgical robot, resonance phenomenon, elastic buckling, optimization, genetic algorithm, FEM.

1. Introduction

Surgical robots are used by doctors to perform surgeries for hard and soft tissues and are used to service artificial organs. So far, many essential constructions of surgical robots have appeared all over the world. The da Vinci construction is the most frequently used robot in clinical practice. Surgical robots end effectors are built with the usage of an open or closed kinematic chain. The most vital parameters of the surgical robot end effector are position accuracy and repeatability. Vibrations have a significant impact on the deterioration of these two parameters of the robot's use during the contact of the tool with the tissue. Also, a negative impact on the robot's motion have the inertia forces of its links, appearing during the velocity changes over time. Due to the inertia forces, it is important to minimize the mass of links of a surgical robot end effector. The objective of this work is to create an optimization model based on four important criteria for mechanics. The first natural frequency that characterizes mechanical resonance is accepted. The buckling coefficient (load factor) determining whether the critical Euler force is exceeded, causing the linear buckling, and the mass affecting the magnitude of the inertia forces. The buckling factor is the quantity by which the applied external force must be multiplied to obtain the value of the Euler force causing linear buckling. The safety factor is also important criterion because it gives the certainty of the safety from the point of view of strength of materials.

It can be said that the optimal design of the surgical robot end effector, due to these four criteria is safe to use and at the same time correct dimensions are achieved, giving the best possible size of the mass system. This article fills an important research gap, which is the lack of a highly complex optimization model (four objective function vector criteria) of a surgical robot effector with such criteria as: mass, natural frequency, buckling coefficient and safety factor.

So far, researchers in various centers around the world have conducted scientific research in this field. For example, topological optimization, the use of the finite element method and the von Mises hypothesis to analyze the stresses of a surgical robot with silicone elements are presented in work [1]. The stress analysis of a surgical robot based on the CAD model and the finite element method as well as structural optimization are described in works [2,3]. The use of Pareto fronts in optimization issues is shown in works [4–7]. Multi-criteria optimization, where the following criteria are adopted: kinematic parameters and stiffness with simultaneous mass minimization when applied to the Delta robot are shown in paper [8]. The

buckling phenomenon for beams and frames was analyzed in work [9]. The work [10] states that the value of the first natural frequency for the PUMA 560 industrial robot used in operations on the human body is 12.5 Hz. The work [11] presents an industrial robot for which the first natural frequency is 10 Hz. The issues related to vibrations and the phenomenon of resonance are analyzed in papers [12, 13]. However, the basics of the finite element method are found in work [14]. Numerical methods of solving eigenproblems are described in paper [15]. Interesting works in the field of construction of surgical robots are [16–21]. The most commonly used construction of the da Vinci medical robot has been described in [22–25].

The effect of this work is the presentation of a structure model for which the resonance frequencies are determined. It is also found that for the load systems occurring in the structure, the linear buckling phenomenon will not occur. At the same time, for safety reasons, it was assumed that the load factor λ should not be lower than 1.5. A limitation on the acceptable stress was also assumed, in the form of a safety factor, and it was accepted that its value should be greater than or equal to 4 for all mechanical elements of the structure of the surgical robot. The calculated extremum of the multi-criteria model created in this way will allow, in the later stages of the design and construction process, to build a prototype of a surgical robot with optimally calculated dimensions and will enable the validation of the obtained numerical results using experimental methods.

2. Methods and Materials

2.1. Experiment on cardiovascular tissue

The research is carried out on a surgical robot end effector model with an open RRRS structure. The structure of the surgical robot end effector has been completed with a scalpel, which enables the operation of a soft tissue. Constant point mechanism (also called RMC – remote center of motion mechanism) with three degrees of freedom, working space and the kinematical chain with 6 degrees of freedom of mentioned surgical robot end effector is illustrated in the figure 1. The RCM is to position the effector in relation to the operated organ inside the patient's body.

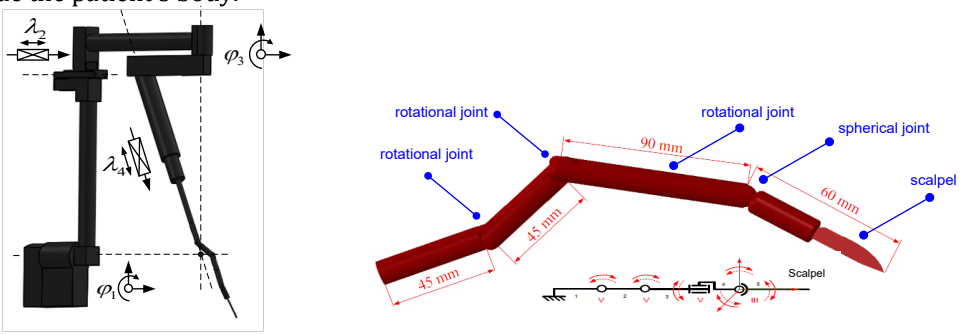

Figure 1. Kinematic chain of surgical robot and surgical robot end effector with open kinematical chain and six degrees of freedom.

A kinematic chain, designed in such a way, enables to reach the back wall of the operated organ and therefore is more useful in certain types of procedures than a chain based on a standard endoscopic instrument with an inelastic sleeve. It also enables the maintenance of an artificial organ after providing the robot's tip with an appropriate tool. Mesh of calculation model, shown in Figure 2 is obtained using the finite element method. The model has 16,730 degrees of freedom. Continuum discretization is completed using the elements of Solid 186. The model is made of aluminum.

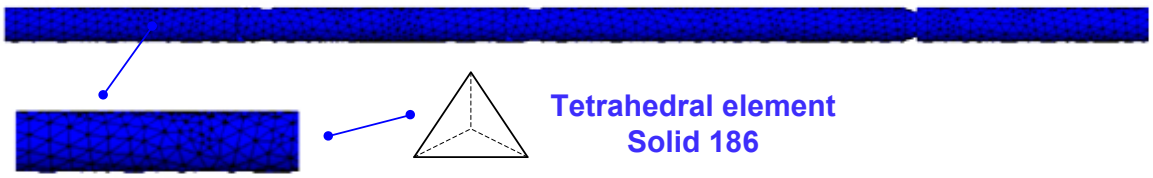

Figure 2. Mesh model of a surgical robot end effector with tetrahedral Solid 186 element.

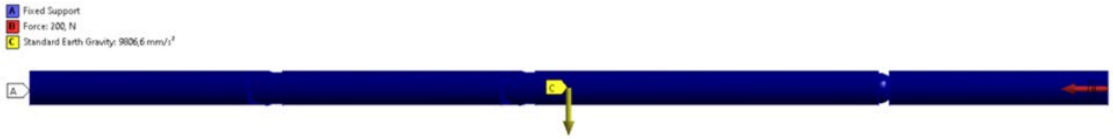

Figure 3. Model of support and load from which the boundary conditions result. Distribution of external forces and the forces of gravity.

A force of 200 N is applied to the model of kinematic chain. Figure 3 demonstrates the nature of support and the application method of loading force. This work is related to eigenvalue problems. In mechanics, there are two important eigenvalue problems, i.e. frequency and buckling. The eigenvalue problem is described by the equation:

$$A \cdot f = \lambda \cdot f, \tag{1}$$

A – square matrix,
f – eigenfunction (eigenvector),
λ – eigenvalue.

In this work, the eigenvalue problems are solved using the finite element method.

2.2. Natural frequency mechanical model

During the operation of a surgical robot end effector, a dangerous phenomenon of mechanical resonance may occur. The work of the robot, in the sections of resonant issues, results in the loss of positioning accuracy. In addition, the robot begins to vibrate strongly, even though the amplitude of the excitation force does not increase. This type of a mechanical resonance is particularly dangerous in case of backlash in robots' kinematic pairs due to its work. Then, structural elements may be overloaded and the structure may be damaged. It is also a threatening situation for the operated patient. The causes of resonance may be the excitations from servomotors, excitations resulting from rotational movements in kinematic pairs, excitations from tissues, e.g. tissue of a heart without stabilization. It is easiest to cause the resonance for the lowest frequency. The resonance plots in the case of damped and undamped resonance are illustrated in the Figure 4. The graphs are interpreted by comparing the frequency of the exciting force with the natural frequency of the robot system. In the case of the damped resonance, it can be observed that the maximum of the graph for the argument of the excitation self-inducting frequency equals to 1.

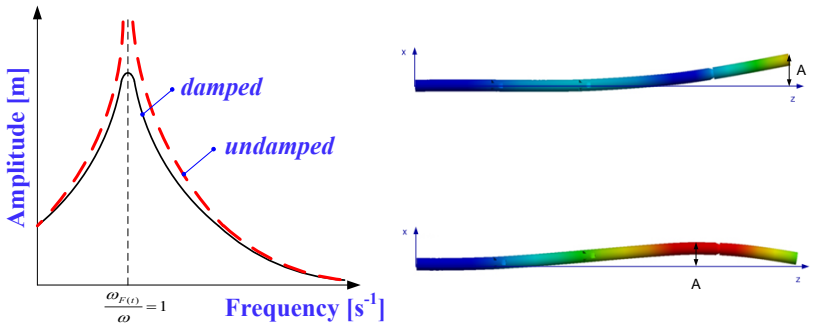

Figure 4. Damped and undamped resonance curve.
Effector resonance shapes with marked A amplitude.

The amplitude of the resonant vibrations is defined as:

$$A = \left|\frac{F_{max}}{m(\omega^2{}_i - \omega^2)}\right|. \tag{2}$$

where: $F_{\max}$– external force N, m – mass kg, ω– external force frequency Hz, ω_i– natural frequency [Hz].

Taking into account the equation of motion assuming no damping, it is possible to characterize an own problem of mechanics with the frequency:

$$[\mathbf{M}] \cdot \{\ddot{\mathbf{u}}\} + [\mathbf{K}] \cdot \{\mathbf{u}\} = \{\mathbf{0}\}. \tag{3}$$

The mass matrix is written as:

$$[\mathbf{M}] = \int_V \rho[\mathbf{N}]^T [\mathbf{N}]dV, \tag{4}$$

where: ρ – density $\frac{\text{kg}}{\text{m}^3}$, $[\mathbf{N}]$ –matrix function shape.

The stiffness matrix $[\mathbf{K}]$ is defined by the equation:

$$[\mathbf{K}] = \int_V [\mathbf{B}]^T [\mathbf{D}][\mathbf{B}]dV, \tag{5}$$

where: $[\mathbf{B}]$–strain- displacement matrix, $\{\boldsymbol{\varepsilon}\}= [\mathbf{B}]\{\mathbf{d}\}$ (matrix function shape), $[\mathbf{D}]$ – constitutive matrix, $\{\boldsymbol{\varepsilon}\}$–strain vector, $\{\mathbf{d}\}$– displacement vector.

The general solution of equation (3) has the following form:

$$\{\mathbf{u}\} = \mathbf{u_A} \cdot \cos(\omega t) + \mathbf{u_B} \cdot \sin(\omega t), \tag{6}$$

$$\{\ddot{\mathbf{u}}\} = -\omega^2\{\mathbf{u}\}. \tag{7}$$

Substituting equation (7) to (3), an equation describing the eigenproblem is obtained with the frequency:

$$([\mathbf{K}] - \omega^2[\mathbf{M}]) \cdot \{\mathbf{u}\} = \{\mathbf{0}\}. \tag{8}$$

where: ω – eigenvalues being as natural frequencies, $\mathbf{u}$ – eigenvector describing the displacement functions during resonance.

2.3 Elastic buckling mechanical model

The differential equation describing the linear buckling problem is formulated as:

$$EJ\frac{d^2y}{dz^2} + Fy = 0, \tag{9}$$

where: E – Young's modulus [Pa], J – moment of inertia [m^4], F – external force [N].
By transforming equation (9) and substituting equation (10) to it:

$$\frac{F}{EJ} = k^2, \tag{10}$$

the following equation is obtained:

$$\frac{d^2y}{dz^2} + k^2y = 0. \tag{11}$$

The general solution of equation (11) has trigonometric form:

$$y = A\cos(kz) + B\sin(kz). \tag{12}$$

Knowing that:

$$kz = \pi, 2\pi, \dots, n\pi, \tag{13}$$

where: $n$is a natural number, Euler's critical force is obtained:

$$F_{cr} = k^2EJ = \frac{\pi^2EJ}{l^2}. \tag{14}$$

The force designated by equation (14) causes elastic buckling in a rod with a length of l m, when any other disturbance is applied to the rod. The system of a straight rob buckled by the Euler critical force F_{cr} is illustrated in Figure 5. The rod was supported on roller and pinned supports.

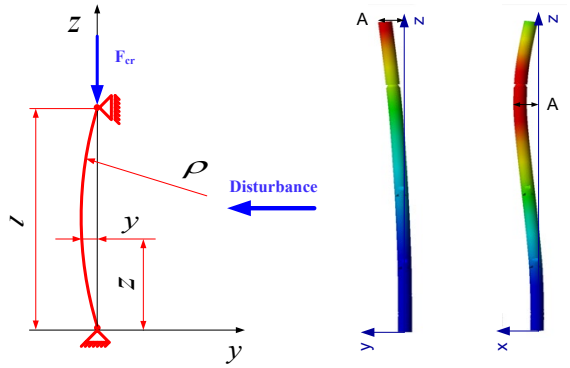

Figure 5. Scheme of linear buckling with Euler force and disturbance. Buckling shapes are illustrated and the amplitudes of deformations are marked.

Assuming that an external force is applied to the rod, it is vital to determine the load factor λ. Euler's critical force value is defined as:

$$F_{cr} = \lambda \cdot F\,. \tag{15}$$

Linear buckling is characterized by the following conditions:

$$\lambda < 1 \text{ – buckling condition (instability)}, \tag{16}$$

$$\lambda > 1 \text{ – stability condition.} \tag{17}$$

If circumstance (16) occurs and any other disturbance is applied, linear buckling appears. However, if the condition (17) occurs, the surgical robot end effector will be a stable mechanical system. The loading factor λ can be calculated by using the finite element method taking into account the static equilibrium and small displacements in the mechanical system. The relationship between the external force and the displacement is written as:

$$[\mathbf{K}] \cdot \{\mathbf{u}\} = \{\mathbf{F}\}, \tag{18}$$

where: $[\mathbf{K}]$ – stiffness matrix, $\{\mathbf{u}\}$– nodal displacement vector, $\{\mathbf{F}\}$ – nodal force vector.

$$[\mathbf{K_G}] = \int_V [\mathbf{G}]^T [\mathbf{S}][\mathbf{G}]dV, \tag{19}$$

where: $[\mathbf{K}_G]$ –stress stiffness matrix, $[\mathbf{G}]$ – matrix obtained from the shape function by differentiation, $[\mathbf{S}]$ – initial stress matrix.

$$([\mathbf{K}] + [\mathbf{K_G}]) \cdot \{\mathbf{u}\} = \{\mathbf{F}\}\,. \tag{20}$$

During the loss of stability for equal loads, other states are possible:

$$([\mathbf{K}] + \lambda[\mathbf{K_G}]) \cdot \{\mathbf{u}\} = \{\mathbf{F}\}, \tag{21}$$

$$([\mathbf{K}] + \lambda[\mathbf{K_G}]) \cdot \{\mathbf{u} + \boldsymbol{\delta}\mathbf{u}\} = \{\mathbf{F}\}. \tag{22}$$

After substituting these equations, a symmetric eigenvalue problem is obtained:

$$([\mathbf{K}] + \lambda[\mathbf{K_G}]) \cdot \{\boldsymbol{\delta}\mathbf{u}\} = \{\mathbf{0}\}, \tag{23}$$

where: λ – eigenvalue vector describing the load factors, $\delta\mathbf{u}$ – eigenvector describing the buckling shapes. In order to solve these problems, the Lanczos method is used for large symmetry problems [26].

2.4 Optimization model with multi-criteria objective function

The MOGA (multi objective genetic algorithm) algorithm NSGA-II is used to calculate the optimum of the multi-criteria objective function. The algorithm is based on Pareto fronts. The Pareto fronts are obtained on the basis of the response surface [27], which are continuous functions acquired from numerical experiments carried out with the finite element method.
The following objective function is adopted.

$$\mathbf{f}(\mathbf{d}) = \{f_1(\mathbf{d}) \longrightarrow \min, f_2(\mathbf{d}) \longrightarrow \max, f_3(\mathbf{d}) \longrightarrow \min,\ f_4(\mathbf{d}) \longrightarrow \min\}. \tag{24}$$

The subsequent restrictions are accepted: $\min \leq d_1 \leq \max$, $\min \leq d_2 \leq \max$, $\min \leq d_3 \leq \max$, 80 [Hz] $\leq f_2(\mathbf{d}) \leq$ 120 [Hz], 1,5 $\leq f_3(\mathbf{d}) \leq 10$, $f_4(\mathbf{d}) \geq 4$. Where: $f_1(\mathbf{d})$ – mass [kg], $f_2(\boldsymbol{d})$– first natural frequency [Hz], $f_3(\mathbf{d})$ – buckling coefficient, $f_4(\mathbf{d})$– safety factor, d_1 – internal dimension of first link [m], d_2– internal dimension of second link [m], d_3 – internal dimension of third link [m].

3. Results

Nature of displacements appearing during the resonance phenomenon for the first four eigenfrequencies of the surgical robot end effector mesh model are illustrated in Figure 6. In the case of the first ω_1 = 114.18 Hz and the second ω_2 = 118.83 Hz of the natural frequency, there are bending vibrations in the longitudinal XZ planes and transverse YZ planes. A similar nature of vibrations is observed for the third frequency ω_3 = 532.21 Hz in the XZ plane and the fourth ω_4 = 541.06 Hz in the YZ plane. Vibrations of this nature are dangerous for the operated patient and contribute to the rapid wear of the surgical robot end effector components, the formation of backlash, jams, and damage.

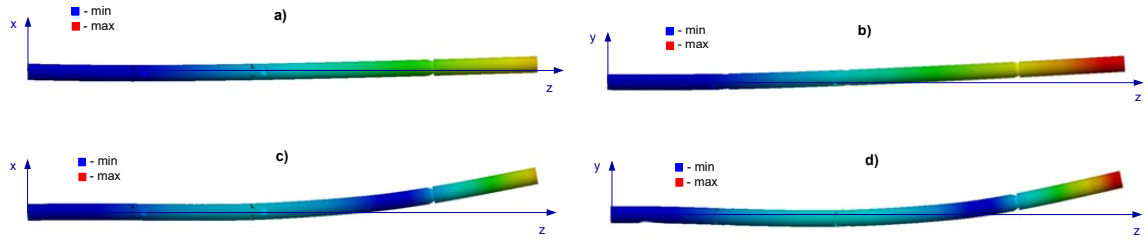

Figure 6. Displacement shapes during resonance for: a) first, b) second, c) third, d) fourth natural frequency.

Nature of the buckling displacements taking place during the linear (elastic) buckling phenomenon for successive values of the load factor λ are shown in the Figure 7. For the first one λ_1 = 2.78 and the other λ_2 = 2.97 values of the buckling (loading) coefficient, periodic displacements occur in the mutually perpendicular planes of the longitudinal XZ and the transverse YZ. The displacements for the third value λ_3 = 15.76 and the fourth λ_4 = 15.97 are of a similar nature.

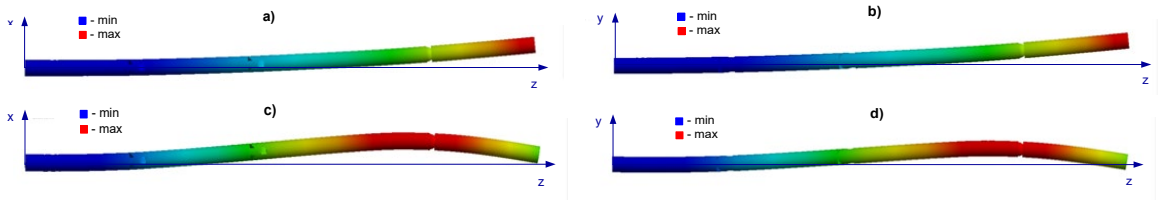

Figure 7. Displacement shapes during linear buckling for: a) first, b) second, c) third, d) fourth value of load factor.

Response surfaces that are metamodels derived from discrete experimental and numerical values after approximation of a continuous function are demonstrate in the Figure 8. Response surfaces are obtained on the basis of numerical data from static structural analysis using FEM, numerical eigenfrequency analysis and buckling analysis with pre-stresses from static analysis. Response surfaces are obtained by the Kriging method.

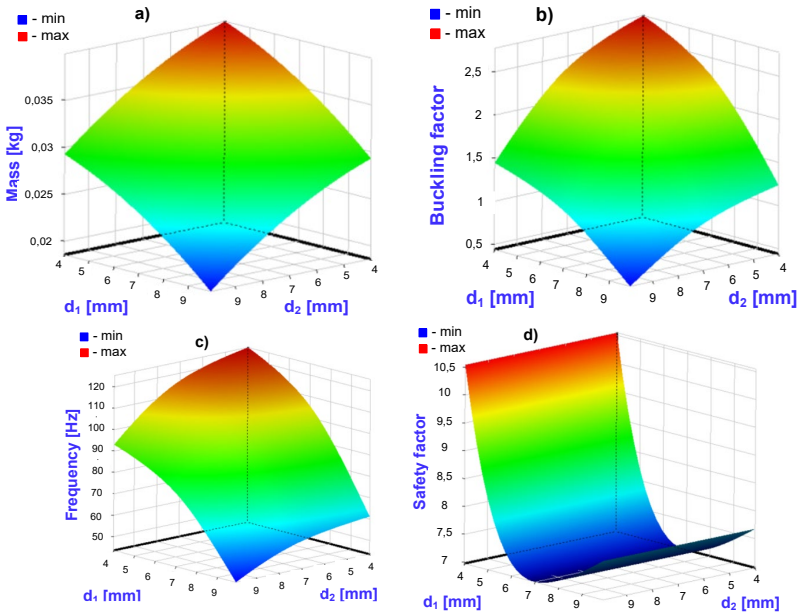

Figure 8. Response surface for: a) mass criterion, b) load factor criterion, c) frequency criterion, d) safety factor criterion.

Based on the meta-models, it is possible to obtain Pareto fronts needed to solve the optimization problem. It is also possible, on their basis, to infer the values of the criteria without the need to conduct an optimization experiment. The Pareto fronts which enable obtaining the optimal result for the vector-valued function of the four criteria are illustrated in the Figure 9. The MOGA (multi objective genetic algorithm) genetic algorithm is used in the variant NSGA-II.

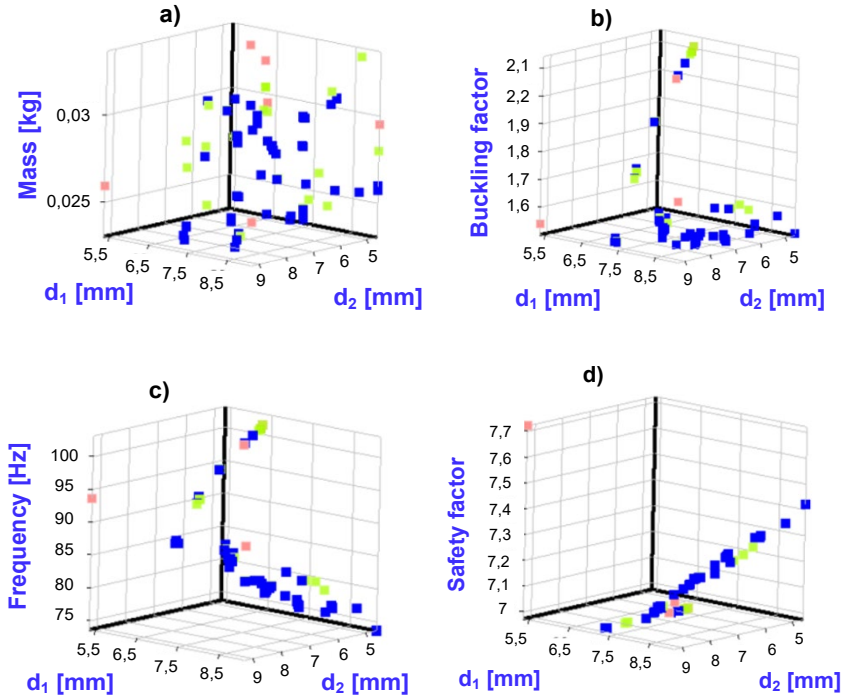

Figure 9. Pareto fronts for: a) mass criterion, b) load factor criterion, c) frequency criterion, d) safety factor criterion.

The multi-criteria function model for four criteria, i.e. mass, first eigenfrequency, buckling coefficient, and safety factor, are solved after 20 iterations using the MOGA genetic algorithm.

Table.1 Values of the arguments of vectorial function and criterions.

Parameter/value	unit
$d_1 = 7{,}77$	mm
$d_2 = 7{,}9$	mm
$d_3 = 9{,}75$	mm
$f_1(\boldsymbol{d}) = 0{,}023$	kg
$f_2(\boldsymbol{d}) = 84{,}84$	Hz
$f_3(\boldsymbol{d}) = 1{,}53$	
$f_4(\boldsymbol{d}) = 7{,}06$	

The following values of geometric quantities are found what is illustrated in the Table 1. For the acquired geometrical dimensions, the optimum values for the objective function criteria are obtained.

4. Conclusions

The outcome of this work is the formulation of an optimization model based on four criteria affecting the effector's position accuracy of a surgical robot end effector. The finite element method turned out to be an effective method of obtaining mechanical data in the form of stresses, values of resonance frequencies, buckling coefficients, safety factors needed to obtain the Pareto fronts of the optimization model. The model made it possible to obtain the best possible values for the adopted criteria under given constraints. The required value of the safety coefficient, safe buckling coefficient and the minimum weight of the robot links are ensured. The minimum value of the mass of links ensures the minimization of inertia forces related to the weight of the robot, thus reducing the deformation of the structure associated with speed changes during functional movements. The value of the first natural frequency, obtained by using the optimization model, equals to 84.84 Hz and provides the required stiffness of the surgical robot end effector structure for the adopted scheme of supports and loads. The forms of resonant vibrations are analyzed and dangerous resonance values are determined, which is the basis for the selection of drive systems. The diagrams of displacements during the linear buckling phenomenon for the assumed boundary conditions are also analyzed. It is noticed that there is no possibility of the linear buckling phenomenon to occur for the assumed load systems. The formulated optimization model also provides the possibility to shape the characteristics of mechanical phenomena based on the geometrical dimensions of the robot's structural elements. In case of the occurrence of the phenomenon of resonance due to the emerging excitations, the optimization model is suitable for detaching the surgical robot end effector system from the resonance frequencies by setting frequency limits on the criterion of the formulated objective function.

Additional information

The author(s) declare: no competing financial interests and that all material taken from other sources (including their own published works) is clearly cited and that appropriate permits are obtained.

References

1. L. Sha, A. Lin, X. Zhao; A topology optimization method of robot lightweight design based on the finite element model of assembly and its applications; Science Progress, 2020, 103, 1–16
2. A. Roya, T. Ghosh, R. Mishraa, S.Kelmash; Dynamic, FEA analysis and optimization of a robotic arm for CT image guided procedures; Materials Today: Proceedings, 2018, 5, 19270–19276
3. T. Ghosh, A. Roya, T. Ghosha, R. Mishraa, S. Kelmash; Structural optimization of a CT guided robotic arm based on static analysis; Materials Today: Proceedings, 2018, 5, 19586–19593
4. R. Konietschke, T. Ortmaier, H. Weiss, R. Engelke, G. Hirzinger; Optimal Design of a Medical Robot for Minimally Invasive Surgery; 2. Jahrestagung der Deutschen Gesellschaft für Computer- und Roboterassistierte Chirurgie (CURAC), Nürnberg, November 4-7, 2003
5. M. Miroir, Y. Nguyen, J. Szewczyk, S.Mazalaigue, E. Ferrary, O. Sterkers, A. Grayeli; RobOtol: from design to evaluation of a robot for middle ear surgery; The 2010 IEEE/RSJ International Conference on Intelligent Robots and Systems, October 18-22, 2010
6. Miroir M., Szewczyk J., Nguyen Y., Mazalaigue S., SterkersO.: Design of a robotic system for minimally invasive surgery of the middle ear. 2nd IEEE RAS & EMBS International Conference on Biomedical Robotics and Biomechatronics, 2008

7. C. Drouin, A. Pourghodrat, S. Miossec, G. Poisson, C. Nelson; Dimensional optimization of A TWO-ARM robot for single-site surgery operations; ASME 2013 International Design Engineering Technical Conferences and Computers and Information in Engineering Conference, 2013
8. B. Bounab; Multi-objective optimal design based kineto-elastostatic performance for the delta parallel mechanism; Robotica, 2016, 34, 258–273
9. M. Bourezane; Buckling finite element analysis of beams and frame," Proceedings of the World Congress on Engineering, 2012, 1
10. A. Jaber, R. Bicker; A Systematic Strategy to Find the Natural Frequencies of an Industrial Robot, Proc. of the Intl. Conf. on Advances in Mechanical and Robotics Engineering, 42–47, 2013
11. A. Doria, S. Cocuzza, N. Comand, M. Bottin, A. Rossi; Analysis of the Compliance Properties of an Industrial Robot with the Mozzi Axis Approach; Robotics. 2019, 80, 1–19
12. M. Crocker; Handbook of noise and vibration control; Wiley, 2007, 528–45
13. W. Fiebig, J. Wróbel; Energy accumulation in mechanical resonance and its use in drive systems of impact machines; Archives of Civil and Mechanical Engineering, 2020, 30
14. O. Zienkiewicz, R. Taylor, J. Zhu; Finite element method; Its basis and fundamentals; Elsevier, 2013.
15. K. Bathe, E. Wilsont; Solution methods for eigenvalue problems in structural mechanics. International Journal for Numerical Methods in Engineering, 1973, 6, 3–226
16. L. Bostic, S. Lanczos; Eigensolution method for high-performance computers; National Aeronautics and Space Administration Memorandum, 1991, 1–20
17. G. Box, K. Wilson; On the Experimental Attainment of Optimum Conditions; Journal of the Royal Statistical Society B, 1951, 13, 1–45
18. R. Howe, Y. Matsuoka; Robotics for surgery; Annual Review of Biomedical Engineering, 1999, 1, 211–240
19. B. Davies: A review of robotics in surgery; Proceedings of the Institution of Mechanical Engineers H, 2000, 214, 129–140
20. R. Taylor, D. Stoianovici; Medical robotics in computer-integrated surgery*;* IEEE Transactions on Robotics and Automation, 2003, 19, 765–781
21. P. Gomes; Surgical robotics: reviewing the past, analysing the present, imagining the future; Robotics and Computer-Integrated Manufacturing, 2011, 27, 261–266
22. S. Najarian, M. Fallahnezhad, E. Afshari; Advances in medical robotic systems with specific applications in surgery – a review; Journal of Medical Engineering and Technology, 2011, 35, 19–33
23. M. Yang, J. Jung, J. Kim; Current and future of spinal robot surgery; Korean Journal of Spine, 2010, 7 61–65
24. G. Sung, S. Gill; Robotic laparoscopic surgery: a comparison of the da Vinci and Zeus systems; Urology, 2001, 58 , 893–898
25. M. Lerner, M. Ayalew, W. Peine, C. Sundaram; Does training on a virtual reality robotic simulator improve performance on the da Vinci surgical system?; Journal of Endourology, 2010, 24, 67–472
26. M. Kroh, H. El-hayek, S. Rosenblatt; First human surgery with a novel single-port robotic system: cholecystectomy using the da Vinci Single-Site platform; Surgical Endoscopy, 2011, 25, 3566–3573
27. K. Shah, R. Abaza; Comparison of intraoperative outcomes using the new and old generation da Vinci robot for robot-assisted laparoscopic prostatectomy; British Journal of Urology International, 2011, 108, 1642–1645